Electromagnetic Field Targeting Enhancement for Carbon Fiber Reinforced Polymers Induction Welding Application

Mansor Ndiaye, Didier Trichet, Antoine Pierquin, Huu-Kien Bui

Electromagnetic Field Targeting Enhancement for Carbon Fiber Reinforced Polymers Induction Welding Application

Mansor Ndiaye[1,2], Didier Trichet[2], Antoine Pierquin[2], Huu-Kien Bui[2]

[1] Nantes Université, IRT Jules Verne, F-44000 Nantes, France.
[2] Nantes Université, Institut de Recherche en Énergie Électrique de Nantes Atlantique, IREENA, UR 4642, F-44600 Saint-Nazaire, France, mansor.ndiaye@univ-nantes.fr

The induction welding of a stringer on an aircraft fuselage skin with a LSP (Lightning Strike Protection) on the underside of the skin is considered. The presence of LSP makes electromagnetic welding very difficult because it concentrates most of the power induced and is therefore more strongly heated than the stringer-skin interface. A new technic coupled with numerical approach which consists in inserting an electrically conductive material into the tooling in order to modify the magnetic field distribution and limit the power induced in the LSP is presented. A strongly coupled electrothermal 2D finite element analysis (FEA) is developed to optimize the temperature profile. 3D FEA is then carried out in order to validate the optimum design.

***Index Terms*— Carbon Fiber Reinforced Polymers (CFRP), Induction welding, finite element method (FEM), LSP**

I. Introduction

ELECTROMAGNETIC induction is a process allowing contactless transfer of energy between a source and a load. The only working condition being that the receiver is electrically conductive, which is the case for the carbon fibers used in Carbon Fiber Reinforced Polymers (CFRP) composite materials. In the context of the development of composite materials, in particular for the aeronautical industry, electromagnetic induction heating has considerable advantages which can become a technological breakthrough with existing processes. This technic is used in aeronautical field for the welding of CFRP.

In this paper, the modeling of a static welding of a stringer on an aircraft fuselage skin with the presence of a Lightning Strike Protection (LSP) by electromagnetic induction is considered. The LSP is a thin layer of copper covering the aircraft fuselage to ensure protection against lightning [1]. At our working frequencies ($100 - 500\,kHz$), the LSP is heated more strongly than the stringer-skin interface and may generate an overheating of the structure during the welding phase which can cause irreversible destruction. Welding composite materials with the presence of LSP is a real industrial issue.

The authors present a new technic which consists in inserting an electrically conductive material into the tooling in order to limit the power induced in the LSP and to redirect the heat in the area of interest. A strongly coupled 2D electrothermal finite element analysis is developed to optimize this material by first screening the best candidates which are then applied to a 3D model to find the optimal configuration.

II. Welding configuration

The welding configuration is presented in Fig. 1. The stringer is placed on a skin having LSP on its underside. The whole is placed on a classical non-electric and non-magnetic tooling. A U-shaped inductor is placed above the stringer. The skin is a CFRP plate of 15 quasi-isotropic folds with a layup plan (orientation angle of each fold) $[45/135/0/90/90/135/45/\overline{0}]_s$ and the stringer a CFRP of 11 quasi-isotropic folds with a layup plane $[45/135/0/0/0/\overline{90}]_s$. Each fold is 184 μm thick and 0° folds are in $y - axis$ direction. The stringer can be separate in-

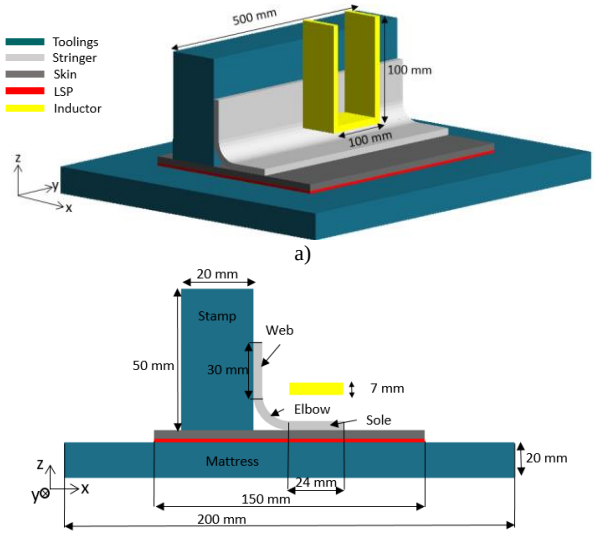

Fig. 1: Welding configuration: a) 3D configuration and b) 2D configuration

to three parts (Fig. 1.b): the sole which is the part to be welded on the skin, the elbow (or radius) and the web (the rise of the stringer). The LSP is a copper grid on the external face of the skin with a thickness of 45 μm. The tooling primarily serves as a support for welding consists of the mattress on which the parts to be welded are placed and the stamp on which the web of the stringer rests to prevent the deformation of the stringer during welding. The choice of the frequency and duration of electromagnetic excitation is very important in static welding. For this type of process, the target cycle time is around 10 s of heating. To achieve the welding objective (melting the sole-skin interface) in this very short time, frequencies of a few hundred kHz are generally applied. The temperature at the interface must then be higher than the melting temperature of the thermoplastic resin ($\sim 380°C$) and lower than its deterioration temperature at the end of the welding process [2]. Therefore, the target temperature T_c to be reached at the interface is set at 400 $°C$. An iterative current calculation loop is then added to the electrothermal coupling loop in order to achieve this temperature for every given configuration.

Fig. 2: Principle of an insert in the mattress

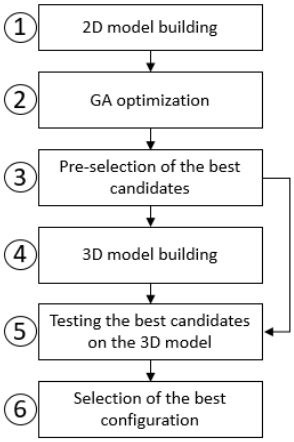

Fig. 3: Different stages of insert optimization

The presence of the LSP in this configuration prevents welding because it concentrates most of the induced heat.

In order to limit the heating of the LSP, an electrical functionalization of the mattress is proposed. It consists of using an electrical conductive insert in the mattress in order to repel the magnetic source field and limit the electromagnetic power induced in the LSP (principle of a magnetic field damper). To be even less dependent on the thermal contact resistance between the LSP and the mattress, the latter is inserted in the mattress and not placed on the surface (Fig. 2). The thickness and optimal position of the insert in the mattress will be determined by a numerical optimization algorithm.

Induction welding involves purely 3D phenomena for many reasons such as the shape of the inductor, the layup plane of the folds or the geometry of the parts. Furthermore, the electromagnetic and thermal properties are strongly nonlinear, anisotropic. A coupled electro-thermal simulation then contains several million unknowns and requires around 3 hours (Intel(R) Xeon E5-1650 3.50 GHz computer with 12 processors) for a typical configuration. It is then impossible to perform an optimization that requires thousands of evaluations of this 3D simulation. The chosen solution in our approach is first to make a pre-selection of some candidates with a 2D model which will take into account all the non-linearities and with a strong coupling, and then to refine the solution with a 3D model restricted to the best candidates (Fig. 3).

III. Electromagnetic and Thermal Formulation

The magnetodynamic $\boldsymbol{A}-\varphi$ formulation [3] is used for the electromagnetic resolution :

$$\begin{cases} \boldsymbol{curl}\dfrac{1}{[\mu]}\boldsymbol{curlA}+[\sigma](j\omega\boldsymbol{A}+\boldsymbol{grad}\varphi)=\boldsymbol{J}^s, & \Omega_{mag} \\ div[\sigma](j\omega\boldsymbol{A}+\boldsymbol{grad}\varphi)=0, & \Omega_{mag} \end{cases} \quad (1)$$

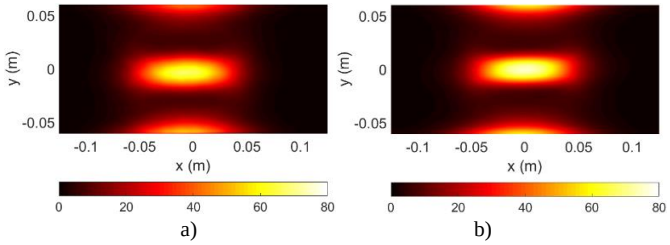

Fig. 4: Thermal image ($°C$) of a) the measurement and b) the model

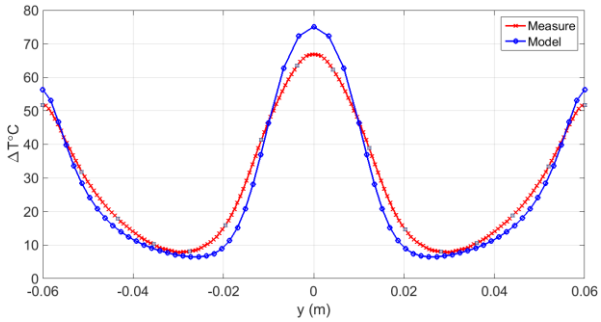

Fig. 5: $\Delta T(°C)$ at $x=0$ of the measurement and the model

where $\boldsymbol{A}$, $\boldsymbol{J}^s$, $[\sigma]$ (which is function of the temperature for the 2D model) and $[\mu]$ are respectively the magnetic vector potential, the source current density, the electrical conductivity tensor. and the magnetic permeability tensor. Ω_{mag} is the electromagnetic domain.

The SIBC (Surface Impedance Boundary Condition) finite element method [4] is used to account for the massive inductor with imposed current source.

$$n\times\boldsymbol{H}|_{\partial\Omega_{ind}}=n\times\frac{1}{\mu}\boldsymbol{curlA}=Z_c^{-1}(n\times\boldsymbol{E})\times n, \quad (2)$$

where Z_c is the surface impedance of the inductor, $\boldsymbol{H}$ and $\boldsymbol{E}$ respectively the magnetic and electrical fields. $\partial\Omega_{ind}$ is the surface of the inductor.

The thermal formulation reads:

$$\begin{cases} -div([\lambda]\boldsymbol{grad}T)+\rho C_p\dfrac{\partial T}{\partial t}=P, & \Omega_{th} \\ -[\lambda]\dfrac{\partial T}{\partial n}=h(T-T_\infty), & \partial\Omega_{th} \end{cases} \quad (3)$$

where $[\lambda]$ is the thermal conductivity tensor, C_p the specific heat, ρ the specific mass and P the induced electromagnetic power density. These parameters are function of the temperature T for the 2D model. T_∞ is the room temperature and the parameter h takes into account the convection h_c and the radiation h_r at the limits of the thermal domain. Ω_{th} and $\partial\Omega_{th}$ are respectively the thermal domain and the limit of the thermal domain. Both electromagnetic and thermal problems are solved by finite element method.

To validate the 3D model, one considers the heating of a 16-folds quasi-isotropic CFRP plate of dimensions $250\times120\times2.35\ mm$ with the following layup plane $[0/45/90/135]_{2s}$. The 0° folds and the inductor are in the direction of the length of the plate. The plate is heated for 5 s with an excitation current of 119 $A\ rms$ and a frequency of 1420 kHz. The air gap is set to 3 mm. Figure 4 shows the thermal images of the meas-

urement and the model obtained on the face of the plate opposite the inductor. One obtains quite similar thermal images. The temperature differences at $x = 0$ of the measurement and the model are plotted in Fig. 5. The comparison shows a good agreement between them.

IV. Optimization of Insert and the Source Parameters

The insert must have optimized thickness and position in the mattress. Then the parameters of the generator (current and frequency) and the position of the inductor (air gap) must allow the target temperature to reach at the interface. Due to the proximity of the inductor to the surface of the sole, the latter can become hotter than the interface. One solution is to force convection at the surface of the sole by means of compressed air nozzles. The value of the convection coefficient h_c required for cooling the surface can be determined by simulation.

A genetic algorithm is then used to find the optimal insert, generator and convection parameters required to achieve the welding objective of maintaining the surface temperature of the sole and LSP below the melting temperature of the resin. Since the current is always calculated through the iterative loop to have a maximum temperature of $400\,°C$ at the sole-skin interface at $10\,s$, a bi-objective function f minimizing the maximum temperature at the sole surface and in the LSP is defined.

$$f(x) = \min_x \left[\max(T^{t_s}_{n_{surface}}(x)); \max(T^{t_s}_{n_{lsp}}(x))\right], \quad (4)$$

where $T^{t_s}_{n_{surface}}$ and $T^{t_s}_{n_{lsp}}$ are respectively the temperatures on the nodes at the sole surface and in the LSP at the end of the electromagnetic excitation ($t_s = 10\,s$), x represents the variables to be optimized.

One adds constraints to avoid excessive temperatures at the surface of the sole and in the LSP:

$$\max(T^{t_s}_{n_{surface}}(x)) < T_{max}, \quad (5)$$

$$\max(T^{t_s}_{n_{lsp}}(x)) < T_{max}, \quad (6)$$

where T_{max} is the maximum temperature allowed at the surface and in the LSP. It is taken to be equal to $600\,°C$.

The variables x to be optimized can be the frequency of the generator, the position of the inductor (air gap), the parameters of the insert (thickness, position and nature), the value of the convection coefficient to apply to the surface of the sole. The choice of variables can be economic or technical (related to the process). For example, the choice of the frequency is directly linked to the limits of the induction generator. The numerical complexity of the optimization problem also depends on the number of variables to be optimized. The choice of these variables must therefore be judicious. It is decided to optimize only 3 variables, namely the frequency f_r, the thickness of the insert e_{insert} and its position in relation to the mattress surface p_{insert}, which are defined as follows:

$$100 \le f_r[kHz] \le 500\,, \quad (7)$$

$$0.1 \le e_{insert}[mm] \le 10\,, \quad (8)$$

$$0.1 \le p_{insert}[mm] \le 10\,. \quad (9)$$

TABLE I
Parameters and Duration of the Optimization

Population size	Maximum number of generations	Total number of evaluations	Total duration ($hours$)
50	100	9956	96.4

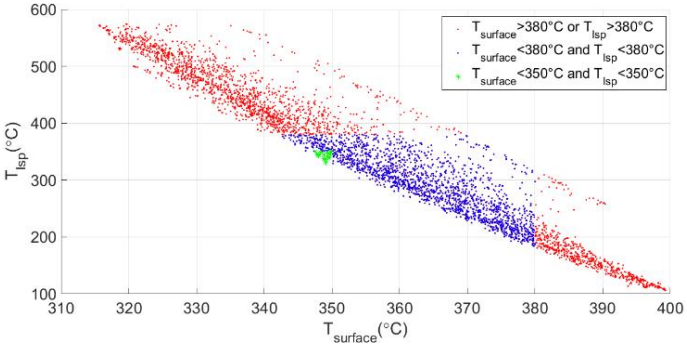

Fig. 6: Maximum temperature in the LSP and on the surface of the sole of the set of configurations generated by the algorithm

TABLE II
Optimal Configurations Found With the 2D Model

Config	f_r (kHz)	e_{insert} (mm)	p_{insert} (mm)	$\max(T^{t_s}_{n_{surface}})$ (°C)	$\max(T^{t_s}_{n_{lsp}})$ (°C)
1	151.83	6.72	0.73	350	345
2	127.61	5.99	0.68	348	344
3	112.14	5.89	0.63	349	331
4	136.34	6.61	0.68	350	338
5	139.03	6.74	0.69	349	341
6	141.53	7.10	0.71	349	345
7	124.13	6.48	0.66	349	336
8	123.85	6.29	0.66	349	337
9	127.22	6.04	0.68	348	344
10	127.77	6.98	0.69	348	345
11	143.24	6.80	0.72	348	349
12	135.17	6.40	0.71	348	350
13	156.15	7.19	0.74	350	348
14	149.84	4.76	0.72	349	347
15	150.37	5.09	0.73	349	348
16	158.54	4.44	0.75	350	350

For the material type of the insert, copper is considered; the air gap is set to $3\,mm$ and the convection coefficient h_c to $150\,W/(m^2K)$ to ensure that the surface of the sole is well cooled.

The optimization parameters of the genetic algorithm and the duration of the simulation are given in Table I. The use of the 2D model allows an analysis on many configurations that would have been impossible with a direct 3D approach.

In Fig. 6, one plots the objectives found on the set of configurations generated by the algorithm. It can be seen that minimizing the surface temperature of the sole maximizes the temperature of the LSP and vice versa. However, there are points that allow both objective functions to be kept below the melting temperature ($380\,°C$) and 16 configurations (Table II) among those that give less than $350\,°C$ at the surface of the sole and in the LSP. One considers these to be the optimal configurations because they offer very interesting process windows that keep the surface of the sole and the LSP away from melting point. The choice of the optimal configuration among these will be

made through a more representative 3D analysis simulation by comparing their thermal responses.

V. 3D WELDING MODEL

One considers a weak electrothermal coupling. The first simulations of this model show that the web of the stringer is heated to high temperatures due to the proximity of the inductor which is just $2\ mm$ away. To limit the heating of the web, the same principle as for the LSP is used by using a magnetic field damper in the stamp to create a feedback field large enough to repel the source field and limit the electromagnetic power induced in the web. The position of the insert in the stamp and its dimensions can also be calculated by an optimization algorithm. However, one considers for the following that it has the same properties (thickness and position) as the insert in the mattress.

The different configurations identified in Table II are evaluated with the 3D model. Very high currents (more than $2000\ A$) are then imposed on the inductor to reach the target temperature at the interface at $10\ s$ of heating because the frequencies are relatively low (a few hundred kHz) on all 16 configurations. The profiles are quite similar to those of the 2D model with some differences in the temperature at the surface of the sole and at the LSP, which is more important with the 3D model. This can be explained by the fact than 3D tensors are used in the 3D model for the definition of the electrical conductivities of the materials in contrast to 2D where only the conductivity in the direction orthogonal to the plane (along the $y-axis$) is imposed for electromagnetic problem. One also notices that in all configurations the maximum temperature at the surface of the sole remains below the melting temperature and the maximum temperature of the LSP exceeds the melting point except for configuration 3 (Table III). The latter would be the optimal configuration since it allows the welding objectives to be achieved. In Fig. 7, thermal image of the 3D model obtained at $10\ s$ heating of the configuration 3 is shown. The temperature in the web of the stringer does not exceed $350\ °C$ and is highest at the top of the latter because this is where the currents looped back. The stringer elbow also stays quite cool after heating is complete. In Fig. 8, the temperatures at the center from the surface of the sole to the mattress with and without insert in the tooling of the configuration 3 are plotted. The comparison shows that without an insert in the tooling, it is impossible to perform welding because the temperature of the LSP greatly exceeds the deterioration temperature of the polymer resin. With the use of an insert, the temperature drops from over $1000\ °C$ in the LSP to less than $380\ °C$. This clearly shows the relevance of the electrical functionalization of the tool because it makes it possible to limit the power induced in the LSP and therefore to control its heating. The insert in the mattress remains cold throughout the welding process, its temperature remains below $50\ °C$.

TABLE III
OPTIMAL CONFIGURATION PARAMETERS

Config	f_r (kHz)	e_{insert} (mm)	p_{insert} (mm)	$\max(T^{ts}_{n_{surface}})$ (°C)	$\max(T^{ts}_{n_{lsp}})$ (°C)	I (A)
3	112.14	5.89	0.63	374.00	373.20	2849

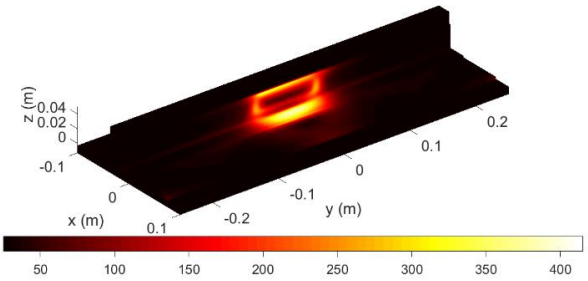

Fig. 7: Thermal image of the 3D model obtained at 10 s heating of the Configuration 3

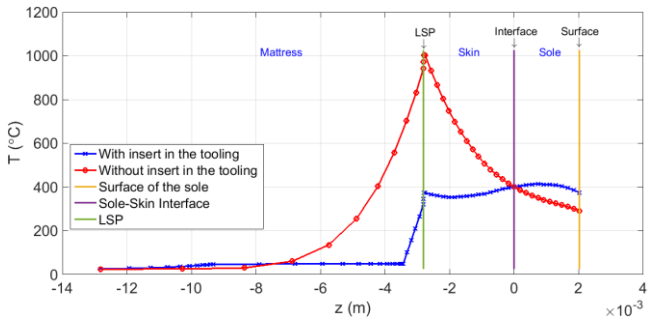

Fig. 8: Temperature at the center from the surface of the sole to the mattress of the configuration 3 with and without insert in the tooling at 10 s

VI. CONCLUSION

The paper presented an industrial problem in the welding of composite materials with the presence of LSP. An original idea of electrical functionalization of the tooling has been presented. It has been shown that the use of an insert with a high electrical conductivity in the tooling can limit the power induced in the LSP and to redirect the heat in areas of interest.

A 2D FEM model coupled with genetic algorithm has been developed in order to optimize the insert's dimensions and the current frequency. This model has allowed for determination of multiple viable solutions during a bi-objective optimization which would be very difficult to obtain with a 3D model. Finally, a 3D model has been developed in order to validate and refine the optimal designs.

ACKNOWLEDGEMENT

This work is part of the PERFORM program managed by IRT Jules Verne (French Institute in Research and Technology in Advanced Manufacturing Technologies for Composite, Metallic and Hybrid Structures).

REFERENCES

[1] J. F. De Toro Espejel and Z. S. Khodaei, "Lightning strike simulation in composite structures," *Key Eng. Mater.*, vol. 754 KEM, no. September 2017, pp. 181–184, 2017.

[2] T. J. Ahmed, D. Stavrov, H. E. N. Bersee, and A. Beukers, "Induction welding of thermoplastic composites — an overview," *Compos. Part A Appl. Sci. Manuf.*, vol. 37, pp. 1638–1651, 2006.

[3] O. Bíró, "Edge element formulations of eddy current problems," *Comput. Methods Appl. Mech. Eng.*, vol. 169, no. 3–4, pp. 391–405, 1999.

[4] A. Ba, H.-K. Bui, D. Trichet, and G. Wasselynck, "Simulation of induction thermography NDT technique using SIBC," *COMPEL - Int. J. Comput. Math. Electr. Electron. Eng.*, vol. 39, no. 5, pp. 1071–1083, 2020.